

a much shorter value would be expected for  $D_1$  of the present complex.<sup>5</sup>

In contrast to the negative indication with respect to a  $D_1$  assignment, an alternative is quite attractive. A one-end dechelated-oxalate species with a water on the vacated-coordination position, as shown in Figure 6, is attractive. In this case,  $\tau'$  would be associated with the rate constants for reclosing of the oxalate chelate ring with substitution for a water ligand. Since it is known that oxoanions form Cr(III) complexes relatively rapidly without fission of a metal-oxygen bond,<sup>14</sup> a value of  $\tau'$  near 1 s would be quite reasonable. This would correspond to a value of  $\epsilon' \approx 10^2$  and  $\Phi' \approx 0.1$ . These are reasonable values since the absorptivity of the aquo-substituted intermediate would be assignable to a ligand-field band similar to those of the starting complex and the quantum yield,  $\Phi'$ , is for a process similar to  $\Phi_{in}$ .

The aquo intermediate is produced with a large stereospecificity as indicated by the nearly complete suppression of the  $\Phi_2(I)$  path of racemization at high  $I$  and the success of the CPL experiment. Since the second step governed by  $k_f$  is essentially the same as that in the fairly well-studied thermal racemization,<sup>15</sup> we have chosen to associate it with inversion. The opposite stereospecificity is also possible since the results demand only specificity.

The wavelength dependence is the clue to the excited-state origin of the reaction leading to the intermediate on the  $\Phi_2(I)$  path. The yield declines beyond 600 nm, which has been shown to be a characteristic of a number of intersystem-crossing processes in Cr(III).<sup>9-11</sup> The implication is clearly that the  $\Phi_2(I)$  path originates from  $D_1$ .

In addition, Figure 6 suggests that the reaction from  $D_1$  leads to a quenchable intermediate (plausibly a doublet). The need for this suggestion is that the ground-state "quenching" shown in Figure 5 promotes racemization. That is, it quenches an initial product to a state farther advanced on the reaction coordinate. The ground-state quenching also excludes the possibility of for-

mation of the intermediate from  $Q_1$ . We emphasize that the argument here rests on a single phenomenon that could not be confirmed with other quenchers.

## Conclusions

The overall mechanism of Figure 6 shows *more variety* in a single reaction than any other Cr(III) system that has been studied. Still, all aspects except the interesting, well-documented, intensity dependence and CPL selectivity have precedents in the Cr(III) literature. Nonetheless, there are specific experimental results requiring *at least* this many *distinct* features in the mechanism! What we can do finally is ask whether the particular suggestions here are consistent with our current theoretical understanding of Cr(III) photochemistry.<sup>3,4</sup>

With respect to the  $\Phi_1$  path, the emphasis given here to a *one-step* intramolecular process does not seem entirely consistent with multistep-dissociative models such as the Vanquickenborne-Ceulemans approach.<sup>3</sup> Rather the present results would tend to lend some support to Kirk's conclusion<sup>3</sup> that a one-step associative version of the model would be useful. From the alternative prompt reaction viewpoint developed by Hollebne,<sup>4</sup> the question becomes the nature of the vibration coordinates excited during excitation since they are postulated to determine prompt relaxation options. For the quartet-quartet transition the octapole rule requires the vibronic coupling to involve the bases  $|3t_1u_0\rangle$ , called the buckle mode,<sup>4</sup> or  $|3t_2u_0\rangle$ , called the twist mode.<sup>4</sup> This last mode is just what is required for a twist-type isomerization.<sup>4</sup>

The large stereospecificity in the  $\Phi_2(I)$  path implies that the  $D_1$  state reacts via attack by water in an  $I_a$  associative step. The assignment of the reaction to  $D_1$  suggests the cis-attack stereochemistry of Figure 6 since there is some precedent for trans attack on  $Q_1$ .<sup>3</sup> Thus, the mechanism proposed in Figure 6 agrees with the main lines of thinking about the theory of Cr(III) photochemistry as recently critically reviewed,<sup>3-5</sup> including the latest nuances.

Registry No.  $K(-)_D[Cr(ox)_2phen]$ , 23594-46-9; KCl, 7447-40-7; KI, 7681-11-0;  $K_3[Cr(CN)_6]$ , 13601-11-1.

(14) H. Ogino, T. Watanabe, N. Tanaka, *Inorg. Chem.*, **14**, 2093 (1975).

(15) J. A. Broomhead, N. A. P. Kane-Maguire, I. Lauder, *Inorg. Chem.*, **9**, 1243 (1970).

## Serial Cyclization: Studies in the Mechanism and Stereochemistry of Peroxy Radical Cyclization<sup>1</sup>

A. Nicholas Roe, Andrew T. McPhail,\* and Ned A. Porter\*

Contribution from P. M. Gross Chemical Laboratories, Duke University, Durham, North Carolina 27706. Received June 14, 1982

**Abstract:** In this study two unsaturated hydroperoxides, model compounds for natural rubber, polyunsaturated isoprenoids such as polyprenols, and polybutadiene, were exposed to initiators in the presence of oxygen. The products of these reactions were isolated and found to be cyclic peroxides that could be produced by a series of reactions involving peroxy radical cyclizations followed by trapping of molecular oxygen to form new peroxy radicals.

Autoxidation, the low-temperature reaction between molecular oxygen and hydrocarbons, is one of the most general reactions in organic chemistry. Free radicals are frequently generated in all systems exposed to the atmosphere,<sup>2</sup> and the reaction of these radicals with molecular oxygen to form peroxy radicals is extremely rapid. The formation and subsequent reaction of these

peroxy radicals are key steps in a wide variety of biological and nonbiological systems.

The degradation of rubber, polybutadiene, and isoprenoid natural products such as squalene, ubiquinones, and other prenyl derivatives, etc. involves peroxy radical intermediates.<sup>3-8</sup> Fur-

(1) Abstracted, in part, from the Dissertation of A. Nicholas Roe, Department of Chemistry, Duke University, 1982.

(2) Totter, J. R. In "Oxygen and Oxy-Radicals in Chemistry and Biology"; Rodgers, M. A. J., Powers, E. L., Eds.; Academic Press: New York, 1981; p 1.

(3) Bevilacqua, E. M. *J. Am. Chem. Soc.* **1955**, *77*, 5394.

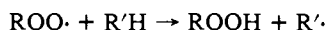
(4) Mayo, F. R. *Ind. Eng. Chem.* **1960**, *52*, 614.

(5) Golub, M. A.; Hsu, M. S. *Rubber Chem. Technol.* **1975**, *48*, 953.

(6) Pecsok, R. L.; Painter, P. C.; Shelton, J. R.; Koenig, J. L. *Rubber Chem. Technol.* **1976**, *49*, 1010.

(7) Shelton, J. R.; Pecsok, R. L.; Koenig, J. L. *ACS Symp. Ser.* **1979**, No. 95, p 75.

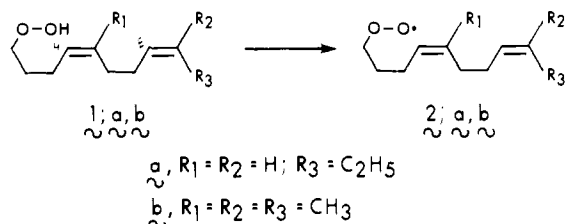
thermore, the role of autoxidation of lipids, especially polyunsaturated fatty acids, in the development of flavors and aromas has been well established.<sup>9</sup> In all of these polyolefin systems, peroxy radicals may undergo intramolecular addition to double bonds and the primary products of oxidation may well be cyclic peroxides.



We report here model studies that establish a multiple cyclization pathway (serial cyclization) in polyolefin oxidation. Serial cyclization would appear to be an important pathway in polyolefin oxidation, and polyperoxides similar to those reported here are potential intermediates in natural product degradation.

## Results

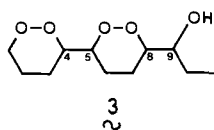
We chose two peroxy radicals for study. Radical **2a** serves as



a model for polybutadiene oxidation while **2b** models peroxy radicals proposed as intermediates in isoprenoid autoxidation. Peroxy radicals, **2**, were generated from the corresponding hydroperoxides, **1**, by hydrogen atom abstraction with *tert*-butoxy radicals, and the hydroperoxides **1a** and **1b** were prepared from the corresponding mesylates by reaction with basic hydrogen peroxide. Methods for preparation of the mesylates and details of their reaction with basic hydrogen peroxide are presented in the Experimental Section. It should be noted that **1a** is a mixture of *E* and *Z* isomers at the  $\Delta^4$  double bond while the stereochemistry at  $\Delta^8$  is only *Z*.

## Autoxidation of 1a

The hydroperoxide **1a** (0.2 M) in benzene (30 °C) under air or pure oxygen was treated with 0.02 radical equiv of *tert*-butoxy radical. The *tert*-butoxy radicals were generated from di-*tert*-butyl hyponitrite (DTBN)<sup>10</sup> or di-*tert*-butyl peroxyoxalate (DBPO).<sup>11</sup> The reaction was terminated when thin layer chromatographic analysis indicated that approximately one-half of the starting hydroperoxide had been consumed. After treatment of the reaction mixture with 1 equiv of triphenylphosphine to reduce hydroperoxides selectively,<sup>12,13</sup> the products were directly separated by high pressure liquid chromatography (HPLC). Four major products, **3a-d**, were isolated in relative ratio 2:2.2:1:1.5. These products were peroxidic, and their <sup>1</sup>H and <sup>13</sup>C NMR spectra (see Experimental Section) as well as C and H analyses were consistent with the proposed structure **3**.



The structure has four chiral centers, allowing a total of eight possible enantiomer pairs, but for clarity and convenience only one enantiomer of each pair will be specified in the following

(8) Bevilacqua, E. M. *Rubber Plast. Age* **1956**, *80*, 271.

(9) Supran, M. K., Ed. *ACS Symp. Ser.* **1978**, *No. 75*.

(10) (a) Mendenhall, G. D. *J. Am. Chem. Soc.* **1974**, *96*, 5000. (b) Kiefer, H.; Traylor, T. G. *Tetrahedron Lett.* **1966**, 6163.

(11) Bartlett, P. D.; Benzing, E. P.; Pincock, R. E. *J. Am. Chem. Soc.* **1960**, *82*, 1753.

(12) Hiatt, R.; Smythe, R. J.; McColeman, C. *Can. J. Chem.* **1971**, *49*, 1707.

(13) Holtz, H. O.; Solomon, P. W.; Mahan, J. E. *J. Org. Chem.* **1973**, *38*, 3175.

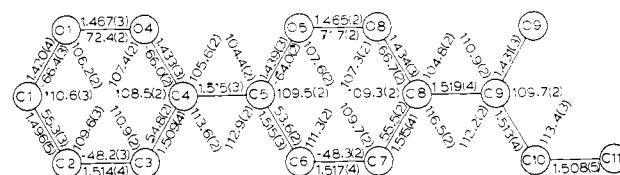


Figure 1. Bond lengths (Å), bond angles (deg), and endocyclic torsion angles (deg) in each of the **3d** molecules.

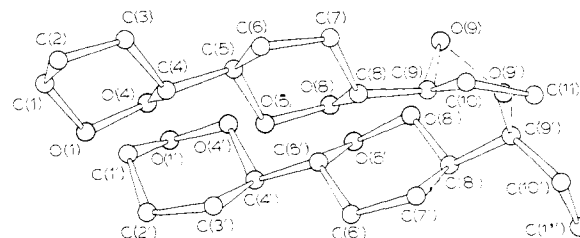
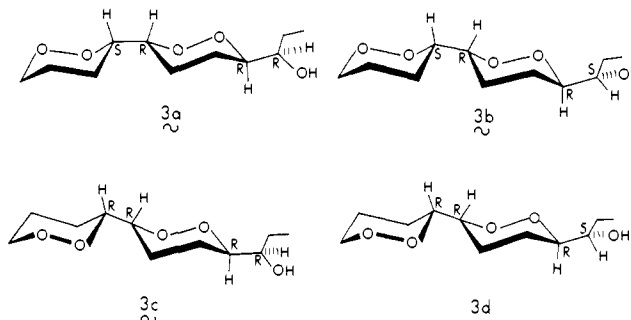


Figure 2. Structure and solid-state conformations of the hydrogen-bonded pair of **3d** molecules defining the asymmetric crystal unit; hydrogen atoms have been omitted for clarity.

discussion. Single-crystal X-ray analyses of two of the four stereoisomers were reported previously,<sup>14</sup> and structural assignments were made as follows: **3a**, 4*S*,5*R*,8*R*,9*R*; **3b**, 4*S*,5*R*,8*R*,9*S*.



Moreover, on the basis of <sup>13</sup>C and <sup>1</sup>H chemical shift comparison of **3c** and **3d** with the firmly defined stereoisomers **3a** and **3b**, we earlier deduced the configurations in **3c** and **3d** to be 4*R*,5*R*,8*R*,9*R* and 4*R*,5*R*,8*R*,9*S*, respectively. We now report confirmation of these latter assignments from the results of a single-crystal X-ray analysis of **3d**.

Crystals of **3d** belong to the triclinic system, space group  $P\bar{1}$ , with four molecules, i.e., two crystallographically independent molecules, in the asymmetric crystal unit. The structure was solved by direct methods.<sup>15</sup> Bond lengths, bond angles, and endocyclic torsion angles are presented in Figure 1.

A view of the solid-state conformation of a pair of **3d** molecules defining the asymmetric crystal unit is provided in Figure 2. These molecules are associated not only by the O(9)–H(9)–O(9')

(14) Porter, N. A.; Roe, A. N.; McPhail, A. T. *J. Am. Chem. Soc.* **1980**, *102*, 7574.

(15) Least-squares refinement of atomic positional and thermal parameters converged to  $R = 0.050$  ( $R = \sum ||F_o| - |F_c|| / \sum |F_o|$ ) over 2777 reflections measured by diffractometer. Non-hydrogen atom positional parameters (Table I), a complete list of torsion angles (Table II), anisotropic thermal parameters (Table III), and hydrogen atom positional and thermal parameters (Table IV) are available as supplementary material.<sup>16</sup>

(16) See paragraph at end of paper regarding supplementary material.

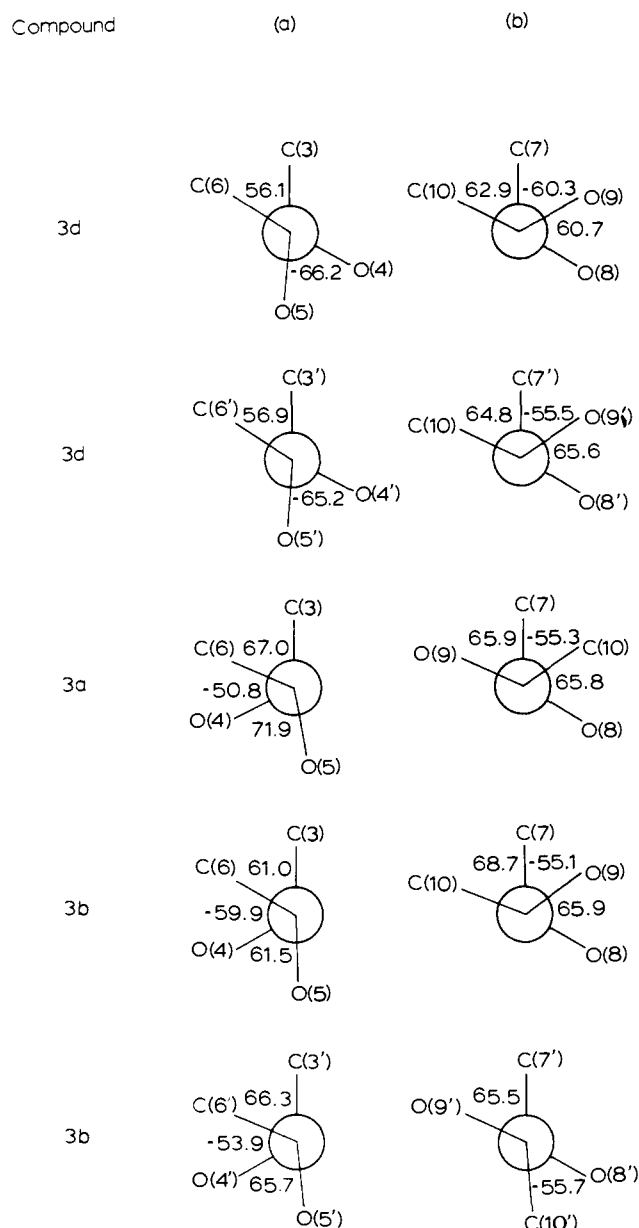


**Figure 3.** Torsion angles (deg) defining the projections along (a) the  $C_4-C_5$  and (b) the  $C_8-C_9$  bonds in **3d**, **3a**, and **3b**.

hydrogen bond  $[O(9)\cdots O(9')] 2.750 \text{ \AA}]$  as shown but also by  $O(9)\cdots H(9')-O(9')$  hydrogen bonds  $[O(9)\cdots O(9') 2.774 \text{ \AA}]$  about crystallographic centers of symmetry. The conformations adopted by both molecules are very similar, with the exception of the terminal methyl group, which is gauche to  $O(9)$  in one molecule but anti in the other, presumably to accommodate the intermolecular hydrogen bonded interactions. Projections along the  $C_4-C_5$  and  $C_8-C_9$  bonds are in Figure 3. In accord with our previous observations on the preferred stereochemistries in this series of compounds, the dioxolane rings in the two crystallographically independent **3d** molecules adopt chair conformations with gauche  $O_4-C_4-C_5-O_5$  orientations and equatorially disposed substituents as in **3a** and **3b**.<sup>17</sup> In contrast, as reference to Figure 3 shows, the  $O_8-C_8-C_9-O_9$  conformation in this series is variable,  $O_8$  and  $O_9$  being gauche in both **3d** molecules as well as in one **3b** molecule but anti in **3a** and the other **3b** molecule. These differences are probably a consequence of the demands of the intermolecular hydrogen bonding and crystal packing effects.

(17) Mean endocyclic bond lengths and dihedral angles in **3a**, **3b**, and **3d** followed: C-C 1.515 (14), C-O 1.440 (12), O-O 1.464 (5) Å; C-C-C 110.3 (10), C-C-O 109.4 (10), C-O-O 107.0 (8)°; C-C-C-C 48.2 (12), C-C-C-O 54.8 (20), C-C-O-O 66.0 (19), C-O-O-C 72.3 (8)°.

**Table V.**  $^{13}\text{C}$  Shifts and Multiplicities<sup>a</sup> of Fractions 4

4a ( $C_6D_6$ )	4b ( $CDCl_3$ )	4c ( $CDCl_3$ )	4d ( $CDCl_3$ )
20.52 q	16.81 t	17.38 q	20.47 q
20.64 t	18.84 t	19.05 t	20.47 t
22.83 t	22.66 t	22.50 t	23.67 t
25.07 t	23.96 t	24.16 t	24.32 t
25.96 q	24.81 q	24.85 q	24.93 q
26.32 q	26.19 q	26.11 q	26.23 q
31.48 t	29.68 t	27.86 t	30.78 t
71.93 s	72.32 s	72.12 s	71.92 s
73.55 t	73.13 t	72.8a t	72.65 t
80.17 s	81.61 s	81.66 s	81.62 s
81.84 d	85.97 d	85.60 d	82.56 d
87.62 d	87.10 d	86.94 d	86.16 d

<sup>a</sup> The multiplicities were determined by off resonance and selective heteronuclear decoupling. Shifts are in units of  $\delta$ .

Despite repeated attempts, it was not possible to obtain crystals of **3c** suitable for X-ray analysis. Nevertheless, confirmation of the predicted structure of **3d** by X-ray and the similarity of  $^1\text{H}$  and  $^{13}\text{C}$  NMR spectra of **3a-d** lend credence to our earlier assignment for **3c**. In fact, each of the diastereomers **3a-d** may adopt conformations where substitution on the  $C_5-C_8$  dioxolane is diequatorial, and the similarity of chemical shifts in  $^1\text{H}$  and  $^{13}\text{C}$  spectra for each isomer is thus anticipated.

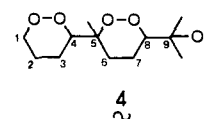
We have isolated a minor component in the reaction mixture, **3e**, that appears to have axial substitution on the  $C_5-C_8$  ring. This diastereomer elutes earlier than **3a-d** on HPLC and is present in less than 5% of the amount of the major isomers **a-d**.

One difference between **3e** and the major isomers can be seen in the 250-MHz  $^1\text{H}$  NMR spectrum. The signal for the protons  $\alpha$  to the peroxide, which appears as a complex pattern from about  $\delta 4.0$  to  $\delta 4.2$  in the major isomers, is much more spread out in **3e** with one hydrogen, represented by a triplet of doublets observed significantly downfield at  $\delta 4.52$ . This suggests that one proton which had been axial in the major isomers is equatorial in **3e**.<sup>18</sup>

The  $^{13}\text{C}$  NMR spectrum also supports the proposed general structure for **3e**. The single absorbance around  $\delta 10$ , the five methylenes from  $\delta 19$  to  $\delta 25$  and the five carbons  $\alpha$  to oxygen from  $\delta 73$  to  $\delta 84$  are characteristic for this series of molecules. It is of interest to note that several of the methylene absorbances are shifted upfield from the corresponding absorbances in the major isomers, suggesting that some of the methylenes may be experiencing some steric compression (see Experimental Section).

#### Autoxidation of **1b**

The hydroperoxide **1b** was treated with 0.02 radical equiv of *tert*-butoxy radical in essentially the same manner as was **1a**. Preparative HPLC of the resultant product mixture, after triphenylphosphine reduction, provided four isomeric products, **4a-d**, in a ratio 1:4.7:4.8:2.2. These compounds gave  $^1\text{H}$  and  $^{13}\text{C}$  NMR spectra consistent with structure **4**. Of these compounds, only



**4a** was submitted for C and H analysis, which was acceptable. For each isomer there is a conspicuous absence of vinyl hydrogens and four protons are observed in the region  $\delta 3.8-4.8$  characteristic of protons  $\alpha$  to peroxides. In the  $^{13}\text{C}$  NMR spectrum, seven signals in the region  $\delta 16-32$  correspond to four methylene and three methyl groups and five signals from  $\delta 71$  to  $\delta 77$  represent those carbons attached to oxygen (see Table V).

There are three chiral centers in **4** at carbons 4, 5, and 8. Therefore  $2^3$  or 8 isomers or 4 pairs of enantiomers may be expected. Since four serial cyclic compounds are isolated from this reaction, they must represent all 4 pairs of enantiomers. These possibilities are as follows: (positions 4, 5, 8) *RRR* (*SSS*); *SRR*

(18) Jackman, L. M. "Applications of Nuclear Magnetic Spectroscopy in Organic Chemistry"; Pergamon Press: New York, 1959; p 115 ff.

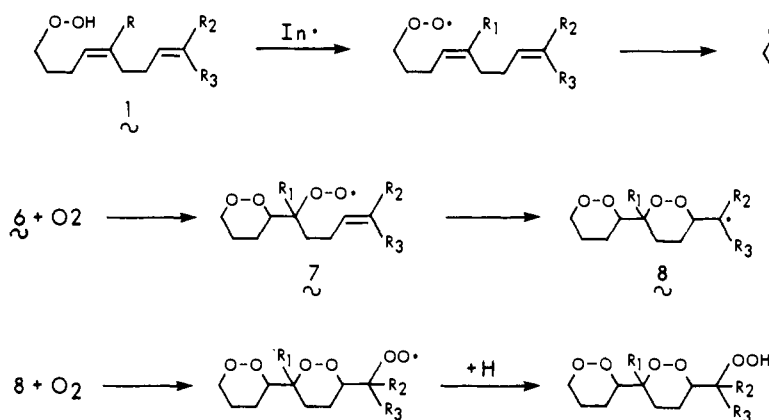
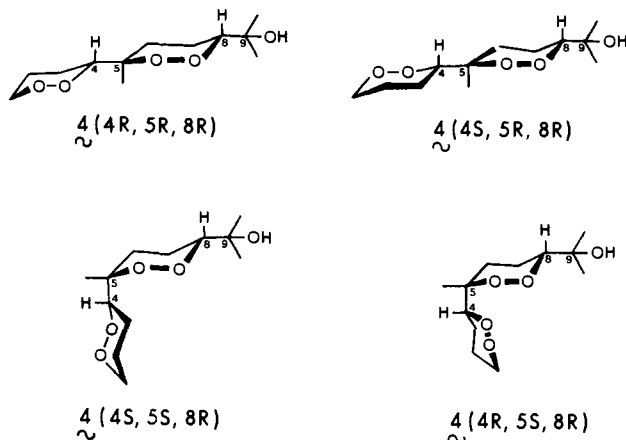


Figure 4. Proposed mechanism for formation of serial products.

(*RSS*); *SSR* (*RRS*); *RSR* (*SRS*).

The four diastereomers of **4** are shown below. The structures

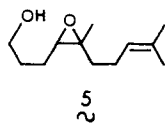


are presented with the bulky  $C(CH_3)_2OH$  group at position 8 in an equatorial position. If this assumption of equatorial substitution at C-8 is correct, then the *SSR* and *RSR* configurations imply that the methyl group at C-5 is equatorial and the dioxanyl group is axial. The *RRR* and *SRR* species have the reverse orientation at C-5.

One result of this isomerism would be a significant shift in the  $^{13}C$  NMR spectrum of the signal for the methyl group attached to C-5, downfield when equatorial, upfield due to steric crowding when axial. There are three carbon signals attributable to methyl groups by selective heteronuclear decoupling. Two are found close together  $\delta$  24.8 and  $\delta$  26.3 in all four isomers. Presumably these two signals result from the two diastereotopic methyl groups attached to C-9. The other methyl signal is found at about  $\delta$  17 in **4b** and **4c** and at  $\delta$  20.5 in **4a** and **4d**, suggesting that in **4b** and **4c** the methyl group on carbon 5 is axial and that it is equatorial in **4a** and **4d**.

We suggest that **4a** and **4d** have *5S,8R* stereochemistry while **4b** and **4c** have *5R,8R* configuration. Thus, from  $^{13}C$  NMR alone we assign stereochemistry for two of the three chiral centers in **4a-d**. We cannot, however, assign the configuration at C-4 with the available data. Unfortunately all efforts to crystallize the serial cyclic compounds **4** failed, as did efforts to derivatize the terminal hydroxy group.

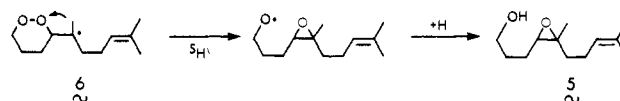
Two other significant products, **5a** and **5b**, may be isolated from the autoxidation product mixture from **1b**. Neither **5a** nor **5b** is peroxidic, and both have resonances in  $^1H$  NMR spectra at  $\delta$  5.07 (1 H, vinylic), 3.7 (2 H, t,  $\alpha$  to OH), and 2.75 (1 H, epoxide H). The  $^1H$  NMR suggests that **5a** and **5b** are the *E* and *Z* isomers of the epoxy alcohol **5**.



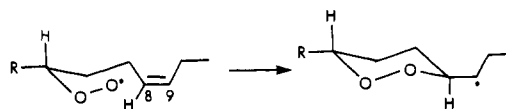
## Discussion

The peroxy radical **2a** serves as a suitable model for radicals formed in the oxidation of polybutadiene, and the isolation of the polycyclic compounds **3** from **2a** establishes serial cyclization as an important mechanistic pathway in polyene oxidation. Product accountability of **3** based on recovered starting material approaches 70%. While we have commented on serial cyclization of **2a** in a preliminary communication,<sup>14</sup> we present here confirmation of the structural assignments of **3c** and **3d** by X-ray analysis (of **3d**), and we report isolation of a new diastereomer, **3e**, that differs from **3a-d** by having *5R,8S* stereochemistry. We also establish the generality of serial cyclization in our studies of **1b** reported here. The radical **1b** serves as a model for peroxy radicals formed in polyisoprenoid autoxidation, and the isolation of the serial cyclic products **4** suggests that polycyclic peroxides may be oxidation products of a host of isoprenoid natural products.

A general mechanism that accounts for isolated products of autoxidation of **1** (**a** and **b**) is presented in Figure 4. Cyclization of peroxy radicals in the 6-exo mode has precedent,<sup>19</sup> and two such cyclizations are suggested in the serial cyclization of **1**. While the serial products **3** and **4** are the major products formed under our conditions of cyclization, we have isolated other products in the cyclization of **1b** that are also consistent with the mechanism outlined in Figure 4. In particular, we find epoxy alcohols **5a** and **5b** that result from  $S_{Hi}$  reaction<sup>20-22</sup> of radical **6**. The fact that



only four of the eight possible pairs of enantiomers of **3** were formed in significant amounts is of mechanistic interest. These four major isomers **3a-d** all have diequatorial substitution on the central ring, suggesting a marked preference for a 1,4-trans-substituted chair conformation in the transition state. The minor isomer, **3e**, reported here must have axial substitution at one of the carbons  $\alpha$  to the peroxide linkage. We estimate that this isomer is formed in less than 5% of the major isomers. Thus, selection of products in 6-exo peroxy radical cyclization can be rationalized on the same basis as product selection is predicted with Beckwith's guidelines<sup>23,24</sup> for 5-exo cyclizations.



(19) Porter, N. A.; Funk, M. O.; Gilmore, D.; Isaac, R.; Nixon, J. *J. Am. Chem. Soc.* **1976**, *98*, 6000.

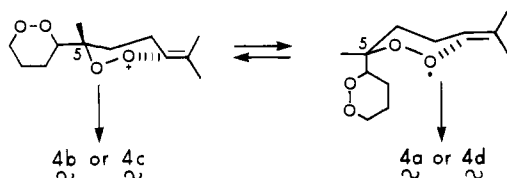
(20) Porter, N. A.; Nixon, J. R. *J. Am. Chem. Soc.* **1978**, *100*, 7116.

(21) Porter, N. A.; Cudd, M. A.; Miller, R. W.; McPhail, A. T. *J. Am. Chem. Soc.* **1980**, *102*, 414.

(22) Nixon, J. R.; Cudd, M. A.; Porter, N. A. *J. Org. Chem.* **1978**, *43*, 4048.

(23) Beckwith, A. L. J.; Wagner, R. D. *J. Am. Chem. Soc.* **1979**, *101*, 7099.

The product selectivity in the formation of **4** is much less



dramatic than that for **3**. The second peroxy radical formed in the serial sequence, **7**, can cyclize via two chair transition states that are much closer in energy than the corresponding radical formed in the cyclization leading to **3**. The ratio of products (**4b** + **4c**)/(**4a** + **4d**) of 9.5:3.2 thus reflects the preference for pseudoequatorial positioning of the dioxolanyl substituent at C-5 in the second peroxy radical cyclization of the sequence.

### Experimental Section

High-performance liquid chromatography (HPLC) was carried out by using a Waters Model M-6000-A pump with a U6K injector. The standard Waters differential refractive index detector was used. A Whatman "Magnum-9" stainless steel column packed with 10- $\mu$ m "partisil" was used for both separation and analysis. "HPLC grade" hexane and isopropyl alcohol obtained from either Burdick and Jackson or Mallinckrodt were used without further purification other than ultrafiltration through Millipore filters. It was important that solvent mixtures be freshly made prior to use for maximum separations. Ethyl acetate was distilled from  $P_2O_5$  and a center cut was used. Thin-layer chromatography was carried out on silica gel 60 precoated glass plates from E. Merck, Darmstadt, Germany. Visualization was achieved by first spraying with a ferrous thiocyanate solution to visualize peroxides. The plate was then sprayed with an acidic solution of ceric ammonium nitrate and heated on a hot plate to show charred organic compounds.

Reagent chemicals were obtained from Aldrich Chemical Co. and purified by standard techniques unless otherwise noted. Benzene was distilled from a blue sodium/benzophenone solution and a center cut was taken.

(24) Beckwith, A. L. J.; Wagner, R. D. *J. Chem. Soc., Chem. Commun.* **1980**, 485.

**Synthesis of Hydroperoxides 1a and 1b.** Details of the synthesis of hydroperoxides **1a** and **1b** are presented in the supplementary material.

**Typical Cyclization Conditions.** The hydroperoxide **1a**, 0.142 g ( $7.16 \times 10^{-4}$  mol), was placed in a dry 50-mL round-bottomed flask and 3.5 mL of distilled benzene was added to make a 0.20 M solution. To this solution 0.0137 g ( $7.155 \times 10^{-5}$  mol) of di-*tert*-butyl hyponitrite was added to give  $1.43 \times 10^{-4}$  mol of *tert*-butoxy radicals or a 0.2 ratio of initiator radicals to hydroperoxide. This solution was either stirred at room temperature or placed in a 30 °C bath under an oxygen atmosphere with magnetic stirring. When approximately half of the hydroperoxide was consumed (by TLC estimate) the solution was cooled to 5 °C and a cold solution of ether containing 0.188 g ( $7.16 \times 10^{-4}$  mol) of triphenylphosphine was added dropwise with stirring. After stirring for 30 min the solvent was stripped and the material injected onto HPLC.

**HPLC Conditions for Products of Cyclization.** Cyclization reaction products were injected into the HPLC in a concentrated ether/hexane mixture. A fresh 4% solution of isopropyl alcohol in hexane at a flow rate of 3 mL per min was found to give good results. The Magnum-9 (Whatman) column required frequent regeneration, even if a guard column was used.

Retention volumes,  $^1H$  and  $^{13}C$  NMR spectra, melting points, and C/H analyses of compounds **3**, **4**, and **5** are given in supplementary material.<sup>16</sup>

**Crystal Data.**  $C_{11}H_{20}O_5$  (**3d**),  $M_r = 232.28$ ; triclinic,  $a = 10.758$  (4) Å,  $b = 13.581$  (6) Å,  $c = 9.018$  (4) Å,  $\alpha = 95.78$  (1)°,  $\beta = 89.86$  (1)°,  $\gamma = 111.92$  (1)°,  $U = 1215$  Å<sup>3</sup>,  $Z = 4$ ,  $d_{calcd} = 1.270$  g cm<sup>-3</sup>; Cu K $\alpha$  radiation,  $\lambda = 1.5418$  Å; absorption coefficient for Cu K $\alpha$  radiation,  $\mu = 8.4$  cm<sup>-1</sup>. Space group  $P\bar{1}(C_1^1)$  from structure analysis and refinement.

Details of crystallographic measurements and structure analysis are presented in the supplementary material.<sup>16</sup>

**Acknowledgment.** This research was supported by grants from NIH (HL 22219) and the National Science Foundation. N.A.P. acknowledges receipt of an NIH RCDA, 1977–1982.

**Supplementary Material Available:** Details for the synthesis of hydroperoxides **1a** and **1b** along with tables of non-hydrogen atom fractional coordinates (Table I), torsion angles (Table II), anisotropic thermal parameters (Table III), hydrogen atom positional and thermal parameters (Table IV), and a list of observed and calculated structure amplitudes (Table VI) for **3d** (36 pages). Ordering information is given on any current masthead page.